

# Catalysis by Metal Ions in Reactions of Crown Ether Substrates

R. Cacciapaglia and L. Mandolini

Centro CNR di Studio sui Meccanismi di Reazione and Dipartimento di Chimica, Università La Sapienza, 00185 Roma, Italy

## 1 Introduction

During the last two decades macrocyclic polyethers have made an impressive impact upon the scientific community,<sup>1</sup> mostly because they have properties in common with the naturally occurring ionophores. They bind alkali and alkaline-earth metal ions, and by virtue of their lipophilic structure are capable of promoting ion extraction and transport in biological and liquid-liquid membranes. The basic concept of the fit between metal ion and macrocyclic cavity size has guided the synthesis of a host of synthetic macrocyclic ligands and, in turn, has stimulated the investigation of the properties of a proportional number of metal complexes.<sup>2</sup> This has led not only to a better understanding of the mechanism of action of the naturally occurring ionophores in biological systems, but has also disclosed novel properties which are interesting *per se* and have been used in a number of useful applications.<sup>1</sup> Among these we have been interested in systems where metal ion complexation by a multidentate ligand is a major factor in controlling the reactivity of the ligand itself. Recognition of the simple principle that coordinative interaction between polyether chains and alkali or alkaline-earth metal ions is an effective force for catalysis led us to the design of simple functionalized crown ethers that were used in studies of metal ion catalysis of acetyl transfer and methyl transfer reactions.

## 2 The Template Effect

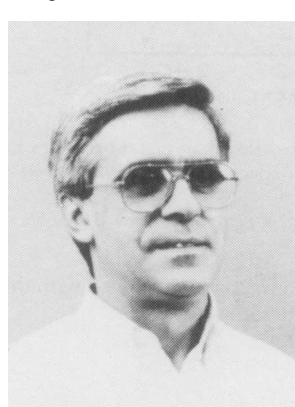
Our earliest interest in crown ethers dates back to the mid-seventies. In those times our group was involved in a thorough research programme on ring-closure reactions of bifunctional chains.<sup>3</sup> The fact that in many reports on the synthesis of crown ethers there were strong indications that ring closure was facilitated by alkali metal ions<sup>4</sup> captured our attention. The very idea that simple and featureless chemical species such as Na<sup>+</sup> or K<sup>+</sup> could enhance rates of macrocyclic ring closure was fascinating. Our kinetic investigations of the template effect in the formation of crown ethers have been briefly reviewed.<sup>5</sup> Hence we will touch here only briefly on some aspects which proved to be relevant to subsequent investigations of metal ion catalysis.

The first approach to the problem was to investigate the influence of added metal ions on the rate of the base-induced closure of B18C6 (*i.e.* benzo-18-crown-6) in water solution from a phenolic precursor having an *ortho* polyether side chain with an  $\omega$ -bromo leaving group.<sup>6</sup> It was soon apparent that the template effect was a kinetically detectable phenomenon. Ring closure was accelerated by Na<sup>+</sup> and K<sup>+</sup>, but not by Li<sup>+</sup> ion. Most strikingly, the divalent ions Sr<sup>2+</sup> and Ba<sup>2+</sup> proved to be even more efficient promoters than the monovalent ones. But more importantly, there was established a powerful technique of kinetic investigation that has been used ever since for our studies on the catalysis and inhibition by metal ions of the reactions of anionic nucleophiles.

More detailed investigations of the template effect were carried out afterwards, both in 99% aqueous Me<sub>2</sub>SO (v/v)<sup>7</sup> and in MeOH.<sup>8</sup> Figure 1 shows the influence of added alkali metal bromides on the first-order rate constant  $k_{\text{obs}}$  for cyclization of the tetramethylammonium salt of *o*-HOC<sub>6</sub>H<sub>4</sub>(OCH<sub>2</sub>CH<sub>2</sub>)<sub>5</sub>Br to B18C6 in 99% Me<sub>2</sub>SO. In these experiments the initial reactant concentration was kept very low (*ca.* 0.1 mmol dm<sup>-3</sup>) in order to make any contribution from second-order dimerization negligible, and to keep to a minimum the amount of metal ions sequestered by the anionic reactant. Known concentrations of metal ions in the kinetic runs were obtained by adding variable amounts of alkali metal bromides, which behave as strong electrolytes in Me<sub>2</sub>SO solution. It is apparent from Figure 1 that all of the metal ions but Li<sup>+</sup> are rate enhancing, and that the magnitude of rate-enhancement is a marked function of cation concentration and nature. The contrasting behaviour of the corresponding set of rate profiles related to the first-order formation of catechol dodecamethylene ether from the parent 12-bromododecyloxy phenoxide (Figure 2) is striking. Here metal ions exert a negative influence in all cases. Strictly similar behaviours were displayed by the intermolecular alkylations of guayacolate and *o*-<sup>-</sup>OC<sub>6</sub>H<sub>4</sub>(OCH<sub>2</sub>CH<sub>2</sub>)<sub>4</sub>OCH<sub>3</sub> with butyl bromide.<sup>7a</sup> Clearly, rate enhancements are only



Roberta Cacciapaglia, born in Rome in 1960, received her laurea degree in Chemistry from the University 'La Sapienza', working in the field of ion pairing effects on reactivity under L. Mandolini. Since 1991 she has been a research fellow of the 'Consiglio Nazionale delle Ricerche' (CNR) at the 'Centro di Studio sui Meccanismi di Reazione', Rome. Her research interests are focused on reactivity and catalysis in supramolecular systems.



Luigi Mandolini, born in Pesaro in 1943, was educated in Chemistry in Rome under G. Illuminati. He began his academic career as an assistant to G. Illuminati (1970—1980) and lecturer in Organic Reaction Mechanisms (1971—1980) at the University 'La Sapienza', Rome, where he has been since 1980 Professor of Organic Chemistry and since 1987 Director of the 'Centro di Studio sui Meccanismi di Reazione' of CNR. He was awarded the 1979 Ciamician Medal of the Organic Chemistry Division of the Italian Chemical Society for his contributions to the field of macrocyclization reactions. His principal research interests lie in physical and mechanistic organic chemistry and supramolecular science.

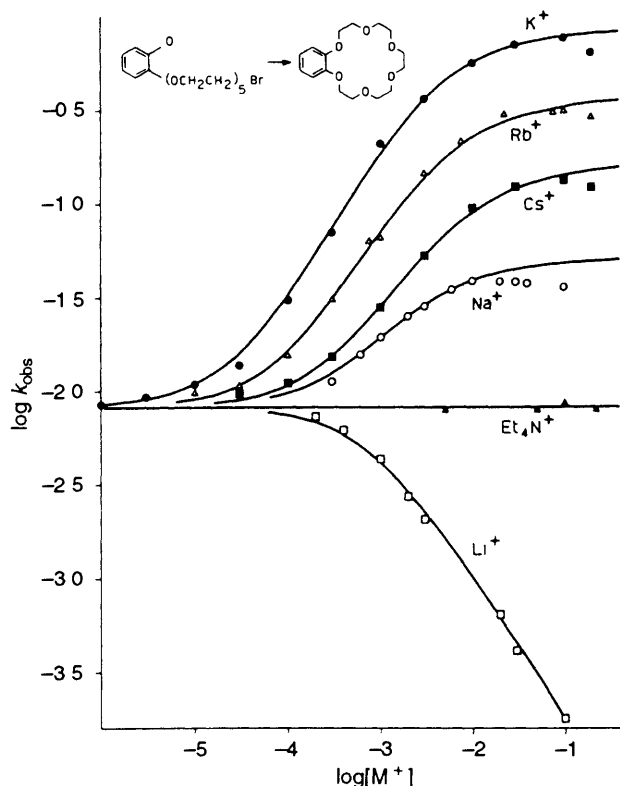


**Figure 1** Effect of tetraethylammonium and alkali-metal bromides on the rate of formation of B18C6 in 99% Me<sub>2</sub>SO at 25.0°C ( $k_{\text{obs}}$  in s<sup>-1</sup>). The horizontal line represents the rate coefficient in the absence of added salts (Reproduced by permission from *J Am Chem Soc.*, 1983 **105**, 555)

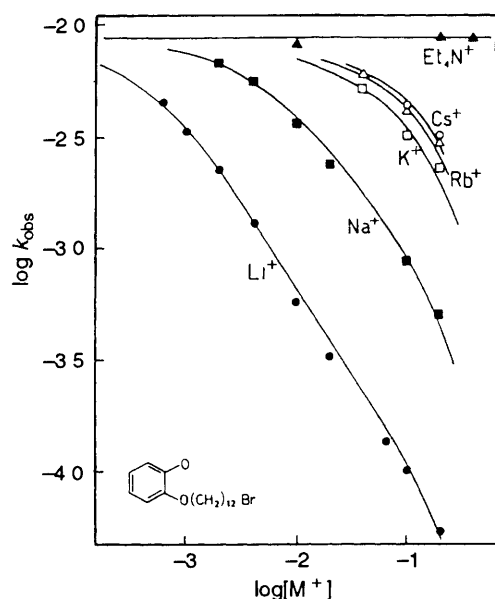


**Figure 2** Effect of tetraethylammonium and alkali-metal bromides on the rate of formation of catechol dodecamethylene ether in 99% Me<sub>2</sub>SO at 25.0°C ( $k_{\text{obs}}$  in s<sup>-1</sup>) (Reproduced by permission from *J Am Chem Soc.*, 1983, **105** 555)

possible when the intramolecular character is combined with the multidentate ligand character in the same system

### 2.1 The Distribution Scheme

Interpretation of the above data in terms of association of the anionic reagent with the alkali metal counter ion, and of

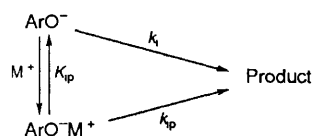


**Figure 3** Distribution scheme according to classical kinetics

independent kinetic contributions from free and cation-paired anions (Figure 3) was suggested, *inter alia*, by the unmistakable saturation behaviour displayed by the profiles of the Na<sup>+</sup>, K<sup>+</sup>, Rb<sup>+</sup>, and Cs<sup>+</sup> reactions reported in Figure 1. The data were accommodated to a good precision by the binding isotherm in equation 1, which is easily derived from the distribution scheme reported in Figure 3, and has the familiar form of a rectangular hyperbola. Since the mean activity coefficient  $\gamma_{\pm}$  was easily calculated from an extended Debye-Hückel equation and  $k_i$  was accurately measured, numerical values for the unknown quantities  $k_{\text{ip}}$  and  $K_{\text{ip}}$  were determined by a non-linear least-square fit of equation 1 to the data

$$k_{\text{obs}} = k_i \frac{1 + (k_{\text{ip}}/k_i)K_{\text{ip}}\gamma_{\pm}^2[M^+]}{1 + K_{\text{ip}}\gamma_{\pm}^2[M^+]} \quad (1)$$

The most interesting feature of the data related to the formation of B18C6 is the fact that K<sup>+</sup> is the best promoter both in 99% Me<sub>2</sub>SO and in MeOH (Table 1). Incidentally, we note that use of MeOH as a solvent permitted determination of the catalytic efficiencies of the alkaline-earth metal ions Ca<sup>2+</sup>, Sr<sup>2+</sup>, and Ba<sup>2+</sup> under the same conditions used for the monovalent ions. The more than 10<sup>3</sup> rate enhancement measured with Sr<sup>2+</sup> was admittedly unexpected, but nevertheless gratifying. It taught us that the amount of binding energy translated into catalysis in reactions promoted by hard metal ions can be very large.

**Table 1** Template effects on the formation of B18C6 in 99% Me<sub>2</sub>SO and in MeOH at 25°C

Metal ion	99% Me <sub>2</sub> SO <sup>a</sup>	$k_{\text{ip}}/k_i$	MeOH <sup>b</sup>
Na <sup>+</sup>	6.1		60.7
K <sup>+</sup>	100		199
Rb <sup>+</sup>	43		48.7
Cs <sup>+</sup>	19		17.1
Ca <sup>2+</sup>			51.6
Sr <sup>2+</sup>			1190
Ba <sup>2+</sup>			334

Data from ref. 7a<sup>a</sup> <sup>b</sup> Data from ref. 8c

### 2.2 The Hole-Size Relationship

When ring sizes other than 18 were considered, ordering among cations changed in a way that was decidedly suggestive of the importance of the match of the metal ions to the cavity of the ring-shaped transition states.<sup>7b</sup> This is clearly shown, for example, by the set of rate profiles related to the formation of B21C7 in 99% Me<sub>2</sub>SO (Figure 4). Clearly, optimum efficiency is obtained here not with K<sup>+</sup>, but with the larger Rb<sup>+</sup> and Cs<sup>+</sup>, the small Na<sup>+</sup> acts as an inhibitor. However, with B15C5, Na<sup>+</sup> turns out to be the best promoter, K<sup>+</sup> ranks next, and Rb<sup>+</sup> and Cs<sup>+</sup> follow in the given order. Not surprisingly, equilibrium constants for association of alkali metal ions to the benzo-crown ether products revealed as a general trend that a metal ion which associates strongly with a crown ether is also a good templating agent in the formation of that crown ether, and that the magnitude of the template effect is basically related to those factors which govern the strength of binding to the reaction product.

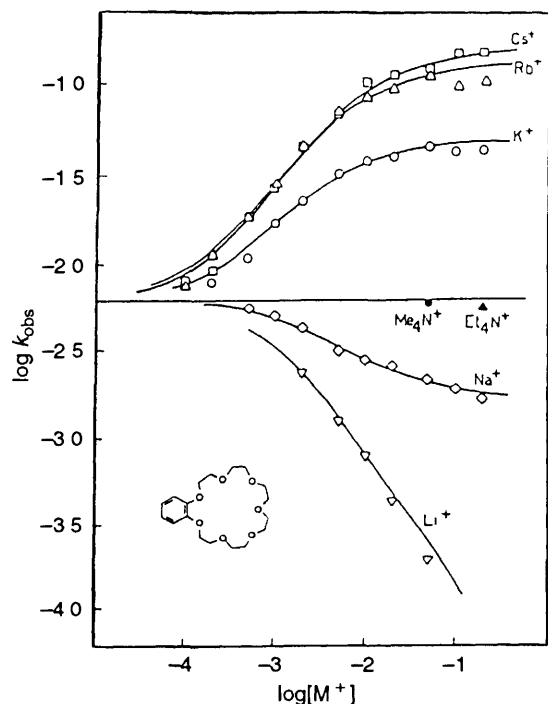


**Figure 4** Effect of tetraalkylammonium and alkali-metal bromides on the rate of formation of B21C7 in 99% Me<sub>2</sub>SO at 25 °C ( $k_{\text{obs}}$  in s<sup>-1</sup>) (Reproduced by permission from *J Am Chem Soc*, 1984, **106**, 168)

### 2.3 Ion Pairing and Reactivity

Inhibition by metal ions, rather than catalysis, clearly occurs for all of the reactions whose rate profiles have a negative first derivative. Figures 1, 2, and 4 show that in all cases, with the sole exception of the Na<sup>+</sup> profile drawn in Figure 4, the curvature is negative, which is a consequence of the fact that the quantity  $(k_{\text{ip}}/k_1)K_{\text{ip}}\gamma_{\pm}^2[\text{M}^+]$  appearing in the numerator of equation 1 is much smaller than unity throughout the investigated concentration ranges and a good fit of the data is obtained with the simplified equation 2. In these cases the only productive route is the free ion pathway, the ion pair being totally unreactive. In contrast, for the Na<sup>+</sup> profile drawn in Figure 4 an inflection point occurs in the neighbourhood of 0.01 mol dm<sup>-3</sup>, above which the curvature becomes positive and the data tend to saturation. This is a clear consequence of the fact that there is an increasingly greater contribution from the ion pair pathway, which renders the quantity  $(k_{\text{ip}}/k_1)K_{\text{ip}}\gamma_{\pm}^2[\text{M}^+]$  significant with respect to unity in the high metal-ion concentration region. For the case at hand,  $k_{\text{ip}}/k_1$  turned out to be 0.27

$$k_{\text{obs}} = \frac{k_1}{1 + K_{\text{ip}}\gamma_{\pm}^2[\text{M}^+]} \quad (2)$$

When we started our studies of the template effect, the notion that ion pairs are less reactive than free ions in S<sub>N</sub>2 reactions was well established.<sup>9</sup> We soon realized, however, that knowledge in the field was based mainly on evidence that was either qualitative or semiquantitative in nature. In addition to the scarcity of ion-pairing constants available in the literature, severe limitations to such studies are ascribable to the serious difficulty of a meaningful separation of ion pair from free ion contributions to the overall rate, particularly when  $k_{\text{ip}}$  is much smaller than  $k_1$ . But we also realized that we had developed a useful technique for the investigation of ion pairing effects on reactivity.

The basic feature of the technique is that the relative proportions of cation-associated and unassociated nucleophile are varied over a wide range by virtue of the mass law effect exerted by varying amounts of added strong electrolytes. As a consequence, ion pairing effects on rates become so large that their recognition is easier and their assessment considerably more

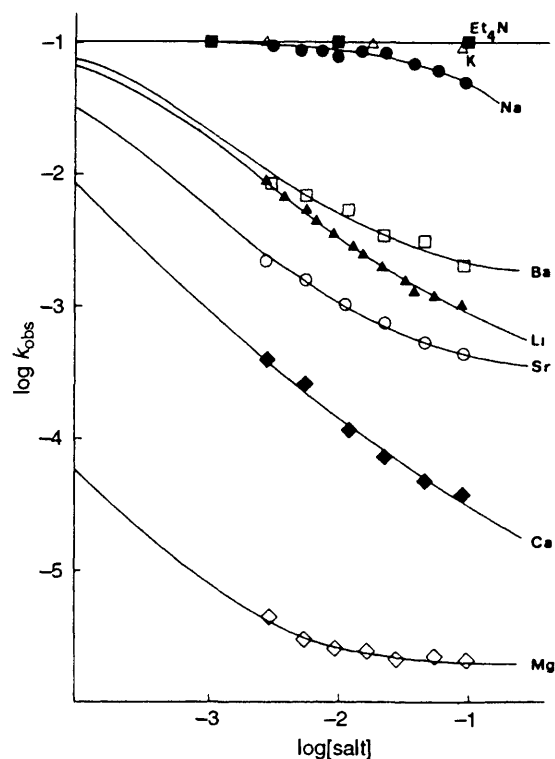
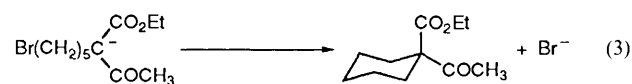


**Figure 5** Effect of tetraethylammonium and metal salts on the rate of intramolecular C-alkylation of the anion of ethyl (5-bromopentyl)acetoacetate in 99% Me<sub>2</sub>SO at 25 °C ( $k_{\text{obs}}$  in s<sup>-1</sup>) (Reproduced by permission from *J Org Chem*, 1988, **53**, 2579)

precise. In practice, the mere occurrence of an inflexion point in a rate profile with negative first derivative may be taken as convincing evidence for the occurrence of significant contributions from the ion pair pathway. Self-consistency is another feature of our technique, which does not rely upon ion pairing constants from other sources, but can in fact be considered a valuable tool for the determination of ion pairing constants. In addition to phenoxides,<sup>7a-10a</sup> our self-consistent approach has been applied to ion pairing effects on alkylation reactions of carboxylates<sup>10b</sup> and malonates,<sup>10c</sup> and to C-<sup>10d</sup> and O-alkylations<sup>10e</sup> of acetoacetic ester derivatives. Although the main goal of this short review article is not the discussion of these studies, a glance at the rate profiles plotted in Figure 5 will suffice to illustrate the potential of the technique. The reaction under investigation is the intramolecular alkylation of the anion derived from ethyl (5-bromopentyl)acetoacetate (equation 3). Analysis of rate data by means of equation 1 showed that  $k_{\text{ip}}/k_1$  is  $4.0 \times 10^{-3}$  for Li<sup>+</sup>,  $1.6 \times 10^{-2}$  for Ba<sup>2+</sup>,  $3.0 \times 10^{-3}$  for Sr<sup>2+</sup>,  $1.0 \times 10^{-4}$  for Ca<sup>2+</sup>, and  $1.7 \times 10^{-5}$  for Mg<sup>2+</sup>.



### 2.4 The Caesium Effect

A brief comment on the so-called caesium effect is in order here. The term refers to the supposedly beneficial influence of Cs<sup>+</sup> compared with the smaller alkali metal ions in alkylation reactions of anionic nucleophiles and, notably, in their intramolecular versions leading to macrocyclic compounds.<sup>11</sup> This notion has been challenged.<sup>12</sup> No special property of Cs<sup>+</sup> emerges from our studies but, rather, a situation where its influence on rates is very similar to those of its next congeners K<sup>+</sup> and Rb<sup>+</sup>, as clearly shown, for instance, by the data plotted in Figure 2. Furthermore, lactonization of 11-bromoundecanoic acid in the presence of alkali metal carbonates revealed a close correspondence between ion pairing effects on lactonization, as

disclosed by the kinetics and yields of the 12-membered lactone. It was concluded that the myth that  $\text{Cs}^+$  favours macrocyclization by directing the reaction in an intramolecular fashion, possibly *via* a 'rolling mechanism' at the surface of the large  $\text{Cs}^+$  ion,<sup>11</sup> was based on little data and some imagination.

### 2.5 Ion Triplets and the Two-metal-ion Pathway

The reactivity and UV spectra of aryloxy ions in DMF are affected by the addition of either  $\text{Li}^+$  or  $\text{Na}^+$  ions in a way that suggests the occurrence of weak ion triplets  $\text{M}^+\text{A}^-\text{M}^+$  in addition to free ions and ion pairs.<sup>10a</sup> Weak ion triplets of the same kind were also detected in DMF with carboxylate ions.<sup>10b</sup> In  $\text{Me}_2\text{SO}$  solution these phenomena are hardly noticeable because of its high dielectric constant ( $\text{Me}_2\text{SO}$ ,  $\epsilon_r = 46.7$ ; DMF,  $\epsilon_r = 36.7$ ). In the presence of ion triplets, a more expanded distribution scheme has to be taken into account (Figure 6).

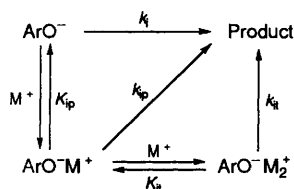


Figure 6 Distribution scheme involving ion triplets.

Whenever both ion pairs and ion triplets are unreactive, as is usually the case, the drop in  $k_{\text{obs}}$  upon increasing  $[\text{M}^+]$  is much steeper than predicted by equation 2. Different situations occur with the templated cyclizations leading to benzo-crown ethers.<sup>10a,13</sup> The influence of increasing amounts of  $\text{KClO}_4$  on the rate of cyclization of  $o\text{-OC}_6\text{H}_4(\text{OCH}_2\text{CH}_2)_6\text{Br}$  to B21C7 in a medium composed of equal volumes of 99%  $\text{Me}_2\text{SO}$  and dioxane is shown by the bell-shaped profile of Figure 7. On increasing the concentration of  $\text{K}^+$  the rate increases first because of the accumulation of the reactive ion pair, but a marked reduction in the extent of catalysis is observed in the high concentration region. This is a consequence of the gradual replacement of the ion pair by the less reactive ion triplet ( $k_{\text{it}} < k_{\text{ip}}$ ). This is not surprising, as there is obviously no room for two  $\text{K}^+$  ions in the cavity of the ring-shaped transition state leading to B21C7. But when the ring becomes larger, as in B30C10, a steep increase in reactivity is found in the concentration region where a reactivity drop is observed with B21C7. This behaviour has been interpreted as being due to the superposition of an additional contribution from the ion triplet, with  $k_{\text{it}} > k_{\text{ip}}$ . It has been suggested<sup>7b,13</sup> that the two  $\text{K}^+$  ions are hosted in the 30-membered ring transition state, as schematically depicted in Figure 8.

### 2.6 Modelling the Transition State

According to transition state theory, equation 1 can be written in the form

$$k_{\text{obs}}/k_i = \frac{1 + K_{\text{T}^\ddagger} \gamma_{\pm}^2 [\text{M}^{2+}]}{1 + K_{\text{ip}} \gamma_{\pm}^2 [\text{M}^{2+}]} \quad (4)$$

where  $K_{\text{T}^\ddagger}$ , operationally defined as

$$K_{\text{T}^\ddagger} = (k_{\text{ip}}/k_i)K_{\text{ip}} \text{ or } k_{\text{ip}}/k_i = K_{\text{T}^\ddagger}/K_{\text{ip}} \quad (5)$$

has the meaning of the formal equilibrium constant for conversion of the transition state which does not contain  $\text{M}^{2+}$  into one which contains  $\text{M}^{2+}$ , *i.e.*, the ion pairing association constant of the transition state (Figure 9).<sup>8c</sup> On the basis of equation 5 the problem of the influence of the metal ion on reactivity resolves itself into questions of the response to the metal ion of the relative ligation abilities of reactant and transition state. This is well illustrated for the template formation of B18C6 in MeOH

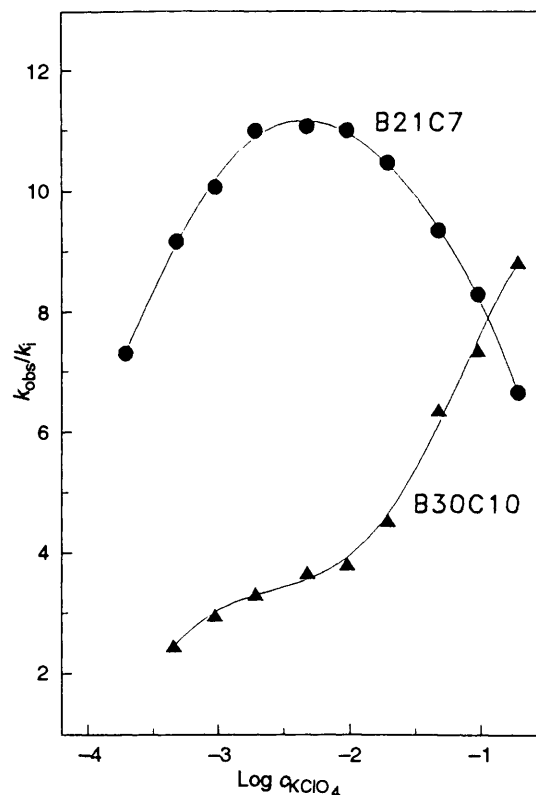


Figure 7 Effect of added  $\text{KClO}_4$  on the rate of formation of B21C7 and B30C10 in dioxane/99%  $\text{Me}_2\text{SO}$  (2:1) at 25 °C. (Data from ref. 13.)

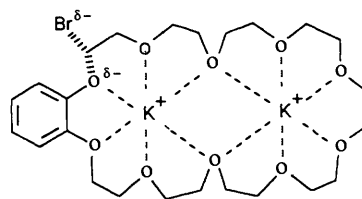


Figure 8 Schematic picture of the transition state for the two-metal-ion pathway in the formation of B30C10.

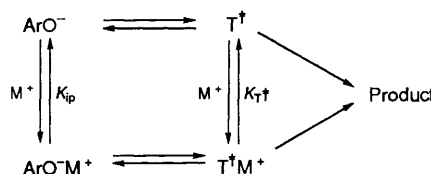


Figure 9 Distribution scheme according to transition state theory.

by a comparison of  $K_{\text{T}^\ddagger}$  values calculated from rate data with equilibrium constants for association of the metal ions with the three polyether ligands involved in the reaction, namely,  $\text{ArOH}$ ,  $\text{ArO}^-$ , and B18C6 (Figure 10). These are all sexadentate oxygen ligands, but belong to different structural types. The open-chain ligands  $\text{ArOH}$  and  $\text{ArO}^-$  differ in the presence of the negative charge that is responsible for the increased complexation power of the latter. On the other hand, the cyclic nature of B18C6 is clearly responsible for its being a much stronger ligand than its acyclic counterpart (a macrocyclic effect). Figure 11 clearly shows that the transition state  $\text{T}^\ddagger$  is the best ligand out of the four species  $\text{ArOH}$ ,  $\text{ArO}^-$ , B18C6, and  $\text{T}^\ddagger$  for all of the given metal ions. This is understandable, since  $\text{T}^\ddagger$  is both cyclic and negatively charged. The effect of the variation of cation on the stability

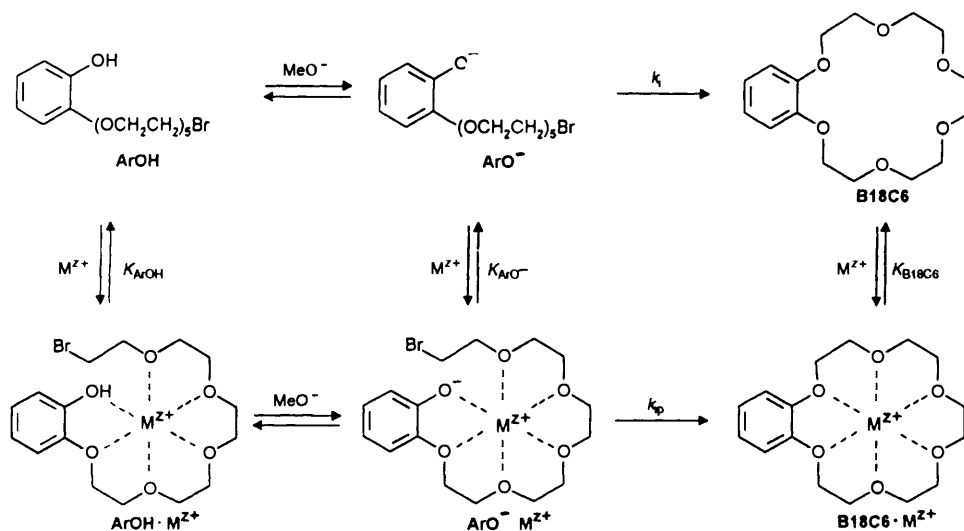


Figure 10 Distribution scheme involving fully coordinated structures.

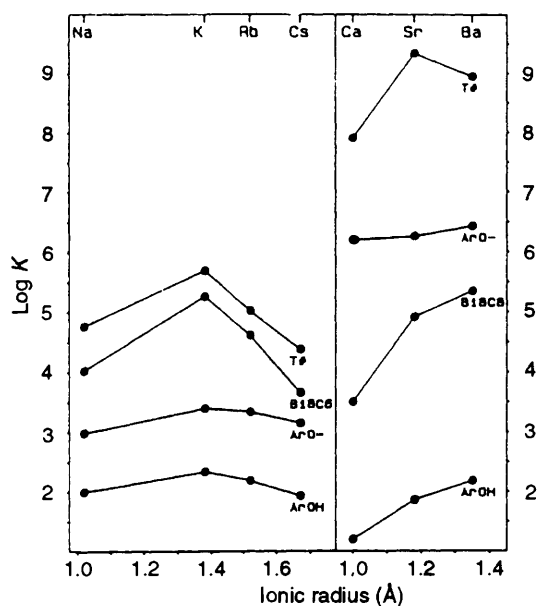


Figure 11 Log  $K$  for association of metal ions with the sexadentate oxygen ligands involved in the B18C6-forming reaction in MeOH solution.

of the  $T^*M^{2+}$  complexes roughly parallels the corresponding effect on the stability of the  $B18C6 \cdot M^{2+}$  complexes, showing that the geometry of the ring-shaped transition state is close to that of the ring product. We note further that the stabilizing effect of the negative charge is stronger in the reactant state complexes than in the transition state complexes, because the negative charge is essentially localized on the aryloxy oxygen in the former, but significantly more spread in the latter. It appears therefore that a representation of the transition state for the metal-templated formation of B18C6, which is consistent with all of the above data, is one involving a fully coordinated structure (Figure 12).

### 3 The Poly(oxyethylene) Side Arm

The basic ingredients of the transition state complex depicted in Figure 12 are (i) a metal ion, (ii) a (somewhat delocalized) negative charge, and (iii) a poly(oxyethylene) side arm. Transition state stabilization by the metal ion occurs through co-

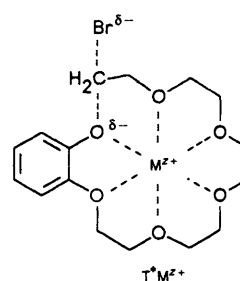
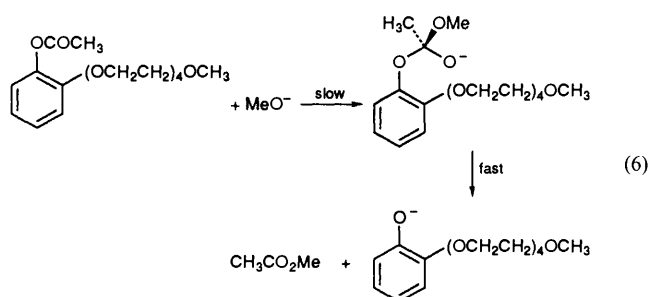


Figure 12 Transition state for the metal-templated formation of B18C6.

operation of electrostatic binding to the negative charge and coordinative binding to the polyether moiety. Now the important question arises as to whether this type of catalysis by alkali and alkaline-earth metal ions is peculiar to crown ether forming reactions or has a more general scope. To answer this question, one should imagine a situation where a polyether moiety is proximal to the negatively charged reaction zone of an anion-neutral-molecule reaction. Unlike the crown ether forming substrates, here the polyether moiety does not bear a reacting group. It should serve the sole, important purpose of providing additional binding sites for complexing the metal ion, thereby increasing the stability of the metal-bound transition state.

### 3.1 Enhancing Rates of Acetyl Transfer

In a first approach to the problem, we have investigated<sup>14</sup> the influence of added alkali (Na, K) and alkaline-earth (Sr, Ba) metal bromides on the rate of acetyl transfer from *o*-acetoxyphenyl 3,6,9,12-tetraoxatridecyl ether to MeO<sup>-</sup> in MeOH at 25 °C (equation 6).



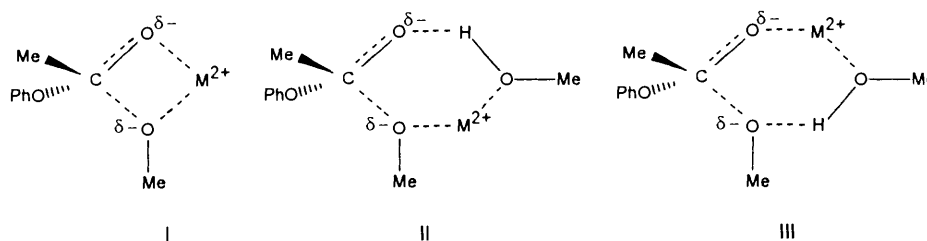


Figure 13 Schematic pictures of the transition state for the metal-ion assisted methanolysis of phenyl acetate

The results largely fulfilled our expectations. All of the added salts increased the rate of reaction according to standard binding isotherms having the general form of equation 4. The order of catalytic efficiency is  $\text{Na}^+ < \text{K}^+ \ll \text{Sr}^{2+} < \text{Ba}^{2+}$ , a maximum rate acceleration of nearly  $10^2$  being observed with the latter metal ion. The finding that the corresponding reaction of the parent phenyl acetate is unaffected by  $\text{Na}^+$  and  $\text{K}^+$ , and accelerated only slightly by the divalent metal ions demonstrates that substantial contributions to the stability of the transition state of the metal-ion assisted path arise from interaction of the metal ion with the oxygen donors of the side arm.

### 3.2 Nucleophilicity of Alkaline-earth Metal Methoxides

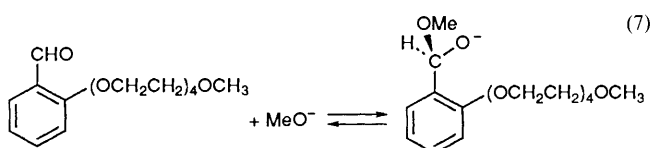
Analysis by means of equation 4 of the rate data obtained in the reactions of phenyl acetate<sup>14</sup> gives  $\log K_{\text{ip}} = 1.78$  and  $1.64$ , and  $\log K_{\text{T}} = 2.45$  and  $2.21$  for  $\text{Sr}^{2+}$  and  $\text{Ba}^{2+}$  respectively. These figures are translated by means of equation 5 into a  $k_{\text{ip}}/k_1$  value of  $4.7$  for  $\text{Sr}^{2+}$  and one of  $3.7$  for  $\text{Ba}^{2+}$ .

A rationale for the finding that the transition state binds  $\text{Sr}^{2+}$  and  $\text{Ba}^{2+}$  more strongly than methoxide ion, in spite of the fact that a more concentrated negative charge is present in the latter, is offered by the chelate structure I (Figure 13) having the form of a four-membered contact ion pair, but it is clear that the six-membered solvent-shared forms II and III are equally consistent with the kinetics.

The fact that the metal-bound methoxide is more reactive than free methoxide is apparently at variance with the widespread belief that ion pairs are less reactive than free ions. This is what is usually observed in nucleophilic substitutions at saturated carbon,<sup>9</sup> but a contrasting behaviour has been recently reported for reactions of carbon-, phosphorous-, and sulfur-based esters.<sup>15</sup>

### 3.3 Enhancing Equilibria in Hemiacetal Anion Formation

The simple strategy based on the poly(oxyethylene) side arm that has been used to enhance rates can also be used to enhance equilibria. The simplest example is offered by the increase in apparent acidity of  $\text{ArOH}$  (Figure 10)<sup>8c</sup> upon metal ion complexation. An additional example is found in a quantitative study<sup>16</sup> of the influence of alkali and alkaline-earth bromides on the equilibrium for the addition of methoxide ion to 2-(1,4,7,10,13-pentaoxatetradecyl)benzaldehyde in MeOH at 25°C (equation 7). Whereas alkali metal ions have no effect, the apparent equilibrium constant is increased by about 420 and 150 times upon addition of  $0.1 \text{ mol dm}^{-3}$   $\text{SrBr}_2$  and  $\text{BaBr}_2$ , respectively. No effect of this sort is observed with benzaldehyde, for which addition of  $\text{MeO}^-$  turned out to be unaffected not only by alkali but also by alkaline-earth metal salts.



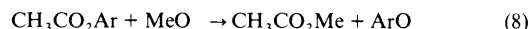
## 4 More Preorganized Substrates

The role of preorganization in host-guest chemistry is well recognized. It is a consequence of the simple principle that conformational changes of the host upon binding to the guest are to be kept to a minimum. Clearly, this condition is poorly fulfilled by the poly(oxyethylene) side arm, on account of its high conformational mobility.

In order to increase the available binding energy and, hopefully, the fraction of this binding energy which can be utilized in catalysis, we have turned our attention to more structured substrates such as macrocyclic polyethers containing a 1,3-xylenyl unit in the macrocyclic backbone, with a functional group X attached to the 2-position of the aromatic ring (Figure 14). The binding properties of these host molecules can be modulated within wide limits by changing the length of the polyether bridge.

### 4.1 Acetyl Transfer Reactions

The effect of alkali (Na, K, Rb, and Cs) and alkaline-earth (Sr, Ba) metal ions on acetyl group transfer to methoxide ion by a series of crown ether acetates, ranging from 2-AcO-15C4 to 2-AcO-27C8 (equation 8), has been investigated in MeOH solution at 25°C.<sup>17</sup> For each substrate a complete set of rate profiles was obtained. An example is shown in Figure 15. In all cases the effect of metal ions is rate enhancing, maximum observed accelerations ranging from 2- to 20-fold with the monovalent ions, and from 2 to 3 orders of magnitude with the divalent ions.



Treatment of rate data for the monovalent ions was carried out by means of equation 9, which is clearly of the same form as equation 4, apart from the  $\gamma_{\pm}^2$  term which does not appear in the numerator of the right-hand side of equation 9 because the experiments were run at constant ionic strength. Here  $k_{\text{obs}}$  is the second-order rate constant measured in the presence of added salt,  $k_0$  refers to reactions run in the presence of tetraalkylammonium ion as the sole counter ion, and  $K_{\text{S}}$  is the equilibrium constant for binding metal ions to the crown ether substrates. The results of the treatment are summarized in graphical form as a plot of  $\log K_{\text{T}}$  vs  $\log K_{\text{S}}$  (Figure 16). It should be noted that the extent of catalysis for each substrate-cation combination is simply given by the vertical difference between the representative point and the origin-intercepting line of unit slope. Not unexpectedly, considerable scatter is apparent in the plot, showing that the relation between binding and catalysis is a complex one. Nevertheless, there is an undeniable tendency for  $K_{\text{T}}$  to increase with increasing  $K_{\text{S}}$ , which indicates that there is a certain degree of resemblance between the altered substrate in the transition state and the unaltered substrate in the reactant state.

$$\frac{k_{\text{obs}}}{k_0} = \frac{1 + K_{\text{T}}[\text{M}^+]}{1 + K_{\text{S}}[\text{M}^+]} \quad (9)$$

In some cases, two metal ions can be accommodated in the macrocyclic cavity of the transition state, giving rise to well defined two-metal-ion pathways, which have been kinetically detected in the  $\text{Na}^+$  and  $\text{K}^+$  reactions of 2-AcO-24C7 and in the

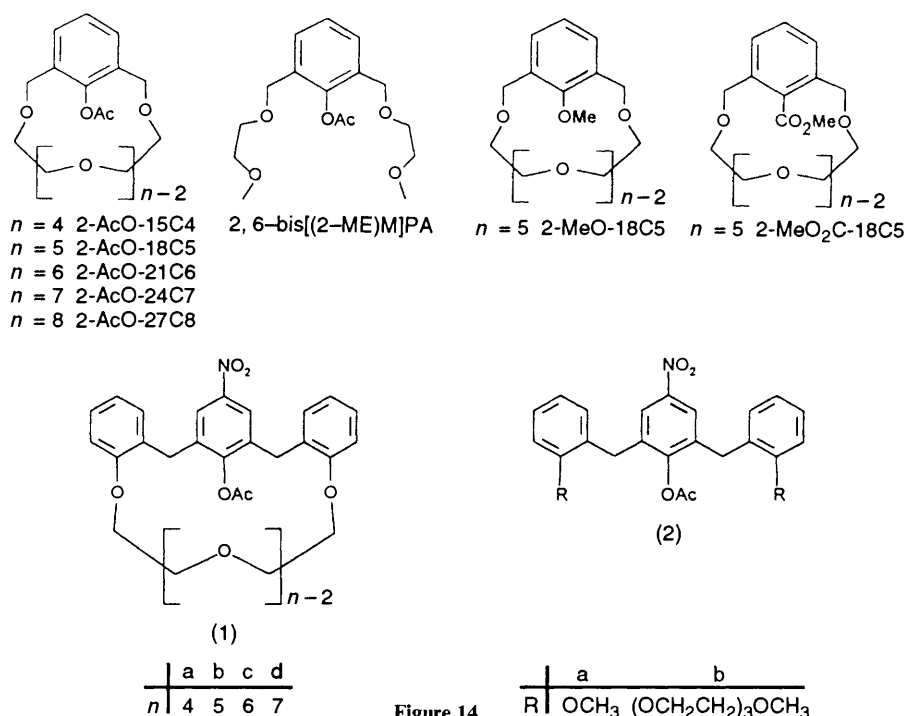


Figure 14

$K^+$  and  $Rb^+$  reactions of 2-AcO-27C8. Thus, there seems to be a close parallel between the two-metal-ion pathway in the templated formation of large ring benzo-crown ethers and the present case. It is worth stressing that the metal ions that can be doubly hosted by 2-AcO-24C7 are  $Na^+$  and  $K^+$ , but for the larger 2-AcO-27C8 it is  $K^+$  and  $Rb^+$  that can be doubly accommodated. No effect of this sort was observed with  $Cs^+$ . These observations point to the existence of a definite correlation between cation size and fit to the macrocyclic cavity.

Treatment of rate data obtained in the presence of  $Sr^{2+}$  and  $Ba^{2+}$  requires an appropriate binomial accounting for association of the metal ion with methoxide to be included in the denominator of equation 9. This leads to equation 10, which fits remarkably well to all of the data. The relevant parameters are summarized in Table 2. The much greater catalytic power of the divalent ions as compared with the monovalent ions is not only

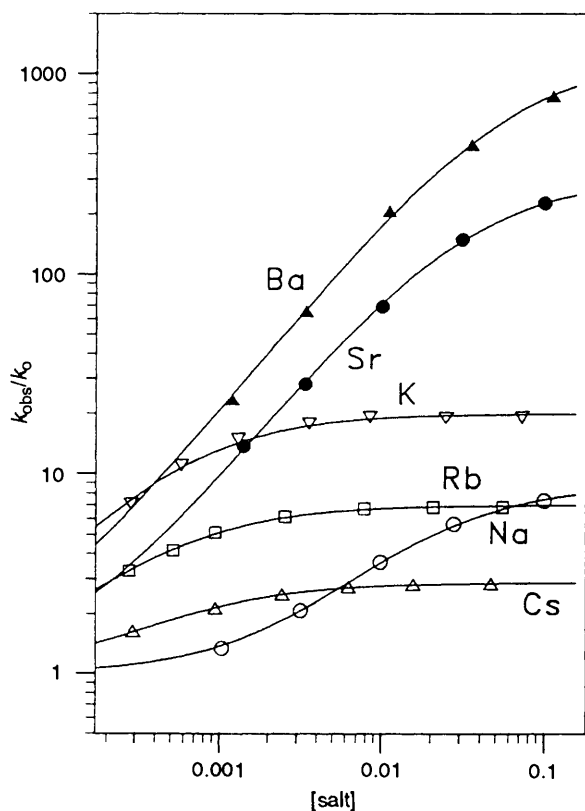


Figure 15 Effect of alkali and alkaline-earth metal bromides on the rate of basic methanolysis of 2-AcO-18C5 at 25°C.

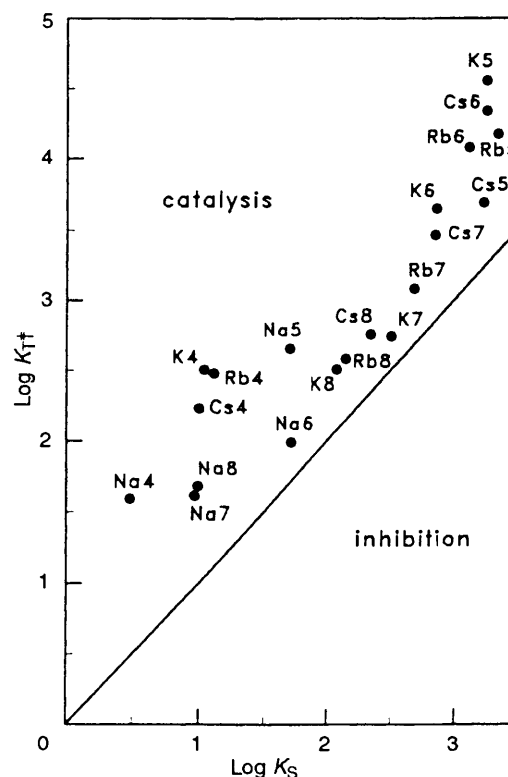


Figure 16 Transition state stabilization vs. reactant state stabilization for the alkali metal ion assisted methanolysis of crown ether aryl acetates 2-AcO-3(n+1)Cn. The numbers attached to the datum points indicate the number of oxygens in the crown ether bridge. The origin-intercepting line of unit slope is the borderline between the catalysis and inhibition domains.

**Table 2** Alkaline-earth metal ion assisted acetyl transfer in MeOH at 25 °C<sup>a</sup>

	$K_S$ (mol <sup>-1</sup> dm <sup>3</sup> )	$K_T^+$ (mol <sup>-1</sup> dm <sup>3</sup> )	$(k_{\text{obs}}/k_o)_{\text{max}}^b$
		2,6-bis[(2-ME)M]PA	
Sr	—	$2.8 \times 10^2$	7.0
Ba	—	$1.7 \times 10^2$	5.6
		2-AcO-15C4	
Sr	—	$1.2 \times 10^3$	$4.0 \times 10$
Ba	—	$2.4 \times 10^3$	$9.3 \times 10$
		2-AcO-18C5	
Sr	—	$9.1 \times 10^3$	$2.3 \times 10^2$
Ba	—	$2.0 \times 10^4$	$7.6 \times 10^2$
		2-AcO-21C6	
Sr	~3	$8.5 \times 10^3$	$1.9 \times 10^2$
Ba	50	$3.2 \times 10^4$	$2.5 \times 10^2$
		2-AcO-24C7	
Sr	8	$2.2 \times 10^4$	$3.5 \times 10^2$
Ba	260	$4.4 \times 10^4$	$1.0 \times 10^2$
		2-AcO-27C8	
Sr	5	$1.3 \times 10^4$	$2.5 \times 10^2$
Ba	74	$2.6 \times 10^4$	$1.6 \times 10^2$

<sup>a</sup>  $K_S$  (mol<sup>-1</sup> dm<sup>3</sup>) for association with methoxide is  $27 \pm 5$  for Sr<sup>2+</sup> and  $19 \pm 4$  for Ba<sup>2+</sup>. <sup>b</sup> Maximum observed rate enhancing effects. Whenever a rate maximum is absent, the rate data refer to 0.1 mol dm<sup>-3</sup> added salt.

due to a much larger electrostatic stabilization of the transition state, but also to a better utilization in catalysis of the binding energy due to coordinative interactions with the polyether bridges. This is clearly shown, for example, by a comparison of data for reaction of the model compound 2,6-bis[(2-ME)M]PA with the corresponding data reported for 2-AcO-15C4 and 2-AcO-18C5. As substrate binding is negligibly small in all cases, the only initial-state stabilization by metal ions which has to be paid for is that of methoxide ion. This means that, unlike the alkali-metal ion reactions of the same substrates, the additional binding energy rendered available in the cyclic substrates, relative to the open-chain model, shows up in the transition states only, and is fully utilized in catalysis.

$$\frac{k_{\text{obs}}}{k_o} = \frac{1 + K_T^+ c_{\text{salt}}}{(1 + K_S c_{\text{salt}})(1 + K_{\text{IP}} c_{\text{salt}})} \quad (10)$$

As a variation on the theme of macrocyclic structures incorporating a 1,3-xylene unit, a series of macrocyclic compounds (1) and open-chain models (2) (Figure 14) incorporating a 2,6-dibenzyl-4-nitrophenyl acetate moiety have been synthesized and tested for Sr<sup>2+</sup> and Ba<sup>2+</sup> catalysis of transacylation.<sup>18</sup> Small rate enhancements were measured in MeO<sup>-</sup>/MeOH, but remarkably high catalytic factors and novel kinetic features were observed in the EtO<sup>-</sup>/EtOH base-solvent system. Evidence was obtained that ethoxide ion is completely bound to the metal ion (equation 11). This leads to a simple kinetic treatment, as the metal-bound ethoxide is treated kinetically as a single species (equation 12). Rate data are summarized in the upper part of Table 3. All of the investigated reactions are promoted by Sr<sup>2+</sup> and Ba<sup>2+</sup>, but it is apparent that more favourable situations are met with the larger macrocycles (1c) and (1d), and with the open chain analogue (2b). These data point once more to the importance of a polyether chain which is available for binding to metal ions, and pose the question as to why the divalent metals are more efficient in EtOH than in MeOH. To answer this, ester cleavage of 2-AcO-15C4, 2-AcO-18C5, and 2-AcO-21C6 was investigated in EtO<sup>-</sup>/EtOH.<sup>19</sup> The rate data listed in the lower part of Table 3 clearly reveal dramatic accelerations by metal ions, the largest effect being displayed by 2-AcO-21C6, which reacts with EtOBaBr half-a-million times faster than with EtONMe<sub>4</sub>. The conclusion was reached that these huge rate enhancements are a consequence of the fact that both electro-

**Table 3** Rate data for acetyl transfer reactions from aryl acetates to ethoxide ion in EtOH at 25 °C<sup>a</sup>

Substrate	EtOSrBr		EtOBaBr	
	$K_S$ (mol <sup>-1</sup> dm <sup>3</sup> )	$k_M/k_o$	$K_S$ (mol <sup>-1</sup> dm <sup>3</sup> )	$k_M/k_o$
pNPOAc <sup>b</sup>	—	8.0	—	7.0
(2a)	—	24.8	—	18.5
(2b)	39	279	25	188
(1a)	—	16.7	—	14.1
(1b)	—	14.2	—	15.1
(1c)	12	46.6	20	91.3
(1d)	11	249	23	691
POAc <sup>c</sup>	—	62	—	45
2-AcO-15C4	48	2 300	54	7 200
2-AcO-18C5	57	48 000	121	46 000
2-AcO-21C6	89	41 000	1 450	500 000

<sup>a</sup> Data from ref. 18 (upper part) and ref. 19 (lower part). <sup>b</sup> pNPOAc = *p*-nitrophenyl acetate. <sup>c</sup> POAc = phenyl acetate.

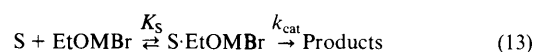
static binding and coordinative binding in the metal-bound transition state are much more efficient in EtOH than in MeOH.



#### 4.2 The Ternary Complex and the Question of Detailed Mechanism

In addition to the exciting crescendo of catalytic factors shown in Table 3, our studies of metal ion catalysis of acetyl transfer in EtOH solution disclosed a kinetic feature that bears directly on the important question of the detailed or microscopic mechanism of catalysis (and inhibition) by metal ions in anion-neutral-molecule reactions.

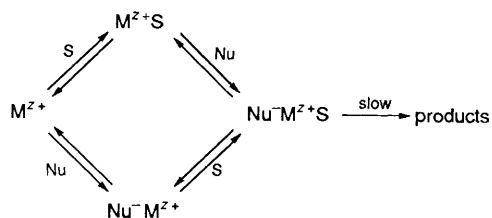
For some of the compounds, plots of  $k_{\text{obs}}$  vs [EtOMBr] were strictly linear over a wide concentration range, but a negative curvature was present in the other cases, which were analysed in terms of the mechanism in equation 13, where the substrate S associates in a reversible fast step with EtOMBr to give what might be called a ternary complex (substrate + ethoxide + metal ion), which decomposes into products in a slow mono-molecular step.



Analysis of rate data for all the compounds showing a non-linear dependence upon [EtOMBr] gave the  $K_S$  values listed in Table 3. Since it seemed unlikely that the fact that some of the substrates follow a certain kinetic equation whereas the others follow a different equation implied a mechanistic change along the series, we assumed that the mechanism of equation 13 applied also to substrates exhibiting linear dependence upon [EtOMBr]. In these cases the ternary complex presumably resembles an inherently unstable random complex, but it is clear from the data in Table 3 that an increasing number of oxygen donors increases the stability of the associated species to the point where a true complex accumulates such as to affect the kinetics.

In general terms, we believe that the dualism between the ion-pair mechanism, in which a cation-paired nucleophile reacts with a free substrate, and the pre-association mechanism, in which a free nucleophile reacts with a metal-bound substrate,<sup>20</sup> can be overcome, at least conceptually, if one assumes that in all cases the reaction proceeds through what, in the language of the enzyme kineticist, is known as a random sequential mechanism (Figure 17). Here the key intermediate is a ternary complex that is formed from reactants and metal ion with no obligatory order of combination.



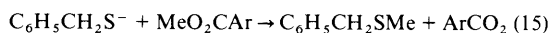
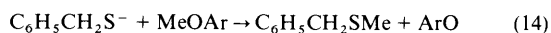

**Figure 17** Random sequential mechanism

From an operational point of view, it should be stressed that here, as in other cases where the reagents are in mobile equilibrium, the question of detailed mechanism, as pointed out by Hammett,<sup>21</sup> is ambiguous because the question is 'In any event it is irrelevant to any presently observable phenomena'. These arguments explain our preference for equation 10 in the treatment of data which, in terms of classical kinetics, are subject to a mechanistic ambiguity<sup>14,17</sup>. Equation 10 is based on transition state theory and, consequently, bears no relation whatsoever to the microscopic or detailed mechanism by which the transition state is attained.

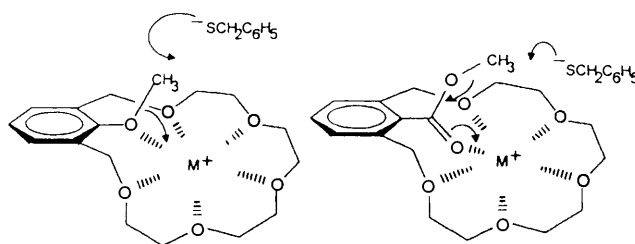
### 4.3 Methyl Transfer Reactions

Metal ion catalysis is by no means restricted to acetyl transfer. Rates of methyl transfer from 2-MeO-18C5<sup>22</sup> and 2-MeO<sub>2</sub>C-18C5<sup>23</sup> to  $\alpha$ -toluenethiolate (equations 14 and 15) are greatly enhanced by alkali metal counter ions in a way that is highly dependent upon the substrate-cation combination (Table 4). When the metal ion is sequestered by cryptand 222, any rate enhancing effect disappears. The crucial role of the crown ether bridge is once again demonstrated by the model compounds 2,6-dimethylanisole and methyl 2,6-dimethylbenzoate, whose demethylation reactions are in fact inhibited, not accelerated, by

alkali metal counter ions. Dissection of metal ion effects into reactant state and transition state contributions was not carried out for these reactions. Nevertheless, there is no doubt that metal-ion binding is strongest in the transition states



Peak reactivity occurs both with 2-MeO-18C5 and 2-MeO<sub>2</sub>C-18C5, but K<sup>+</sup> is the best promoter with the former, and Na<sup>+</sup> with the latter. This seems to be a consequence of the hole-size relationship, as suggested by the naive pictures of the transition states involving fully coordinated structures (Figure 18). The cavity defined by the polyether bridge and the bulkier methoxycarbonyl group is somewhat smaller than the corresponding cavity in the crown ether anisole and, consequently, more suitable to host the smaller Na<sup>+</sup> ion.


**Figure 18** Transition states for the cleavage of 2-MeO-18C5 and 2-MeO<sub>2</sub>C-18C5

We further note that metal ion effects are about an order of magnitude larger in the demethylation of the crown-anisole, which is believed to arise from a stronger electrostatic binding in the metal-bound transition state. Here the negative charge transferred from the thiolate nucleophile is essentially localized on a single oxygen atom, but spread over both oxygens of the methoxycarbonyl group in the reactions of 2-MeO<sub>2</sub>C-18C5.

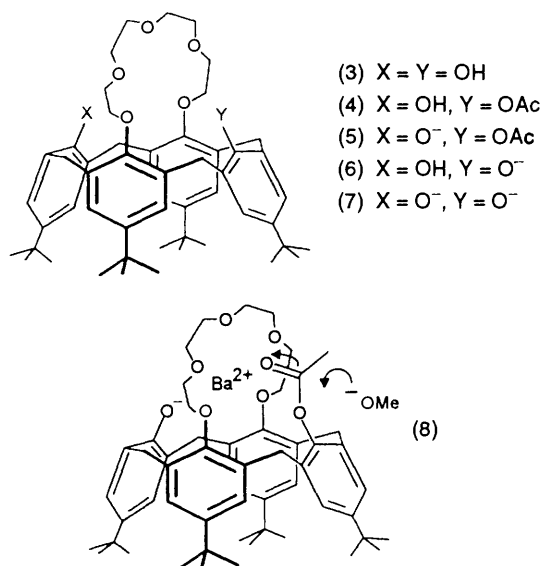
**Table 4** Cleavage of methyl 2,6-dimethylbenzoate, 2-MeO<sub>2</sub>C-18C5, 2,6-dimethylanisole, and 2-MeO-18C5 by C<sub>6</sub>H<sub>5</sub>CH<sub>2</sub>S<sup>-</sup>M<sup>+</sup>

M <sup>+</sup>	<i>k</i> <sub>rel</sub>
Methyl 2,6-dimethylbenzoate <sup>a</sup>	
K <sup>+</sup> [2 2 2]	1 <sup>b</sup>
Li <sup>+</sup>	0.54
Na <sup>+</sup>	0.57
K <sup>+</sup>	0.66
Cs <sup>+</sup>	0.43
2-MeO <sub>2</sub> C-18C5 <sup>a</sup>	
K <sup>+</sup> [2 2 2]	1
Li <sup>+</sup>	1.5
Na <sup>+</sup>	47
K <sup>+</sup>	17
Cs <sup>+</sup>	4.4
2,6-Dimethylanisole <sup>d</sup>	
K <sup>+</sup> [2 2 2]	1 <sup>c</sup>
Li <sup>+</sup>	0.25
Na <sup>+</sup>	0.43
K <sup>+</sup>	0.43
Cs <sup>+</sup>	0.42
2-MeO-18C5 <sup>d</sup>	
K <sup>+</sup> [2 2 2]	1 <sup>f</sup>
Li <sup>+</sup>	26
Na <sup>+</sup>	565
K <sup>+</sup>	826
Cs <sup>+</sup>	146

In DMF (+ 1.6 mol dm<sup>-3</sup> H<sub>2</sub>O) at 35°C. Data from ref. 23.  
 $k = 3.5 \times 10^{-4} \text{ mol}^{-1} \text{ dm}^3 \text{ s}^{-1}$  /  $k = 3.2 \times 10^{-4} \text{ mol}^{-1} \text{ dm}^3 \text{ s}^{-1}$   
 In DMF (+ 3.3 mol dm<sup>-3</sup> H<sub>2</sub>O) at 60°C. Data from ref. 22.  
 $k = 8.9 \times 10^{-7} \text{ mol}^{-1} \text{ dm}^3 \text{ s}^{-1}$  /  $k = 4.6 \times 10^{-7} \text{ mol}^{-1} \text{ dm}^3 \text{ s}^{-1}$

### 5 Acetyl Transfer in Calixarene Systems

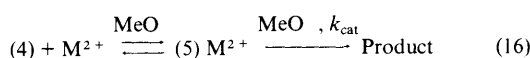
The monoacetylated derivative (4) of *p*-tert-butylcalix[4]arene-crown-5 (3), constitutes a further step toward more preorganized structures (Figure 19).<sup>24</sup> Ionization of the phenolic hydroxyl of (4) has the potential for providing an additional binding site for holding a metal ion in the crown ether cavity very near to the acetoxy group. Deacetylation of (4) in Me<sub>4</sub>NOMe/MeOH


**Figure 19**

occurs very slowly at 25 °C, with a second-order rate constant  $k_{\text{uncat}}$  of  $3.4 \times 10^{-5} \text{ mol}^{-1} \text{ dm}^3 \text{ s}^{-1}$ . By way of an example, the half-life in a  $1 \text{ mmol dm}^{-3} \text{ Me}_4\text{NOMe}$  solution is 34 weeks, but drops astonishingly to 8 s upon addition of  $1 \text{ mmol dm}^{-3} \text{ BaBr}_2$ . Strontium bromide promotes the reaction, but to a somewhat smaller extent. Much lower, yet still remarkable rate enhancements are brought about by monovalent ions. Methanolysis in  $40 \text{ mmol dm}^{-3} \text{ Me}_4\text{NOMe}$  is accelerated 3300-fold by  $40 \text{ mmol dm}^{-3} \text{ KBr}$ , and 220-fold by  $43 \text{ mmol dm}^{-3} \text{ RbBr}$ .

Combination of kinetic and UV spectroscopic data shows that in the absence of metal ions attack of  $\text{MeO}^-$  takes place on the non-ionized form (4), but in the presence of metal ions the reactive form is the metal complex of the ionized form (5), which is present in significant amounts by virtue of the acidity-enhancing effect of the metal ions (equation 16). Thus, the simple replacement of the ionizable proton of (4) with a metal ion converts an unreactive species into a very labile one. The metal ion, hosted in the cavity delimited by the crown ether bridge and the aryloxy oxygen, activates the carbonyl group toward nucleophilic attack, as depicted in (8).

Analysis of rate data showed that  $k_{\text{cat}}/k_{\text{uncat}}$  is  $1.2 \times 10^6$  for  $\text{SrBr}_2$  and  $2.1 \times 10^7$  for  $\text{BaBr}_2$ , which are translated into transition state stabilizations of 8.3 and 10.0 kcal mol $^{-1}$ , respectively (1 cal = 4.184 J). To the best of our knowledge, these are the most striking examples of electrophilic catalysis by these ions.



### 5.1 A Novel Nucleophilic Catalyst with Transacylase Activity

The acidity enhancing properties of divalent metal ions, coupled with their rate-enhancing properties in acyl transfer reactions, can be put to the purpose of developing a nucleophilic catalyst with transacylase activity.

When properly activated by  $\text{Ba}^{2+}$  under mild basic conditions, (3) acts as a transacylation catalyst in the methanolysis of *p*-nitrophenyl acetate (pNPOAc) in a medium composed of 90% MeCN and 10% MeOH (v/v) at 25 °C.<sup>25</sup> The results of a typical set of kinetic experiments are plotted in Figure 20. The slow liberation of *p*-nitrophenol (pNPOH) due to background methanolysis ( $t_{1/2}$  ca 5 days) is unaffected by addition of (3), but significantly accelerated by an equimolar mixture of (3) and  $\text{BaBr}_2$ . The initial burst of pNPOH release is followed by a linear portion where the reaction order is zero and the slope is above an order of magnitude larger than background. The linear portion extrapolates back to an initial burst which corresponds nearly to the initial concentration of (3). The occurrence of a catalyst-substrate covalent intermediate in the catalysis pathway was

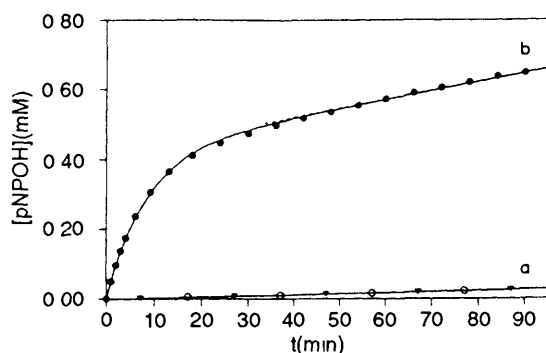


**Figure 20** Appearance of pNPOH during methanolysis of pNPOAc ( $30 \text{ mmol dm}^{-3}$ ) in MeCN/MeOH (9/1) in the presence of diisopropylethylamine bromide salt buffer ( $[\text{B}]/[\text{BHBr}] = 3/1$ ). Curve (a)  $\blacktriangledown$  background reaction measured in the presence of buffer alone,  $\circ$  buffer plus  $0.46 \text{ mmol dm}^{-3}$  (3). Curve (b) buffer plus  $0.46 \text{ mmol dm}^{-3}$  (3)  $0.46 \text{ mmol dm}^{-3} \text{ BaBr}_2$ , the full line is calculated. (Reproduced by permission from *J Am Chem Soc*, 1992, **114** 10956.)

strongly suggested by the phenomenological behaviour typical of ping-pong kinetics,<sup>26</sup> and directly confirmed by HPLC analysis. The turnover number is  $5.5 \times 10^{-3} \text{ min}^{-1}$ , which means a catalyst turn over rate of eight times per day.

In the presence of  $\text{Ba}^{2+}$ , about 1/6 of (3) is in the form of the neutral barium complex (7)  $\text{Ba}^{2+}$ , the rest being probably in the form of (6)  $\text{Ba}^{2+}$ . The kinetics indicate that the active form of the catalyst is the barium complex of the doubly ionized form (7), and that the entire catalytic cycle takes place as shown in Figure 21. In the active complex (7)  $\text{Ba}^{2+}$ , the negative poles and the polyether bridge act as working units that perform cooperatively in providing the driving force for the formation of the complex itself, and the barium ion serves as an electrophilic catalyst both in the acylation and in the deacylation steps.

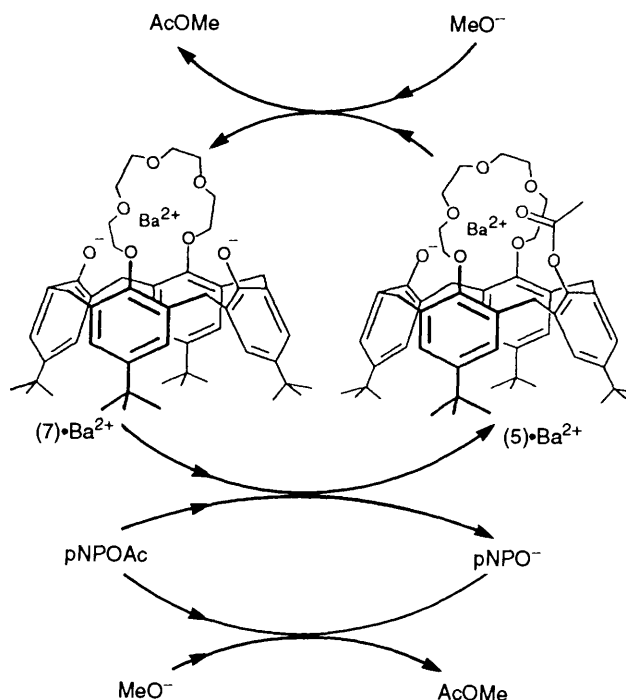


**Figure 21** The barium salt of (3) as a nucleophilic catalyst with transacylase activity.

The design and synthesis of organic catalysts that possess some of the attributes of enzymes is a major challenge in supramolecular chemistry. Much work has been done on synthetic catalysts with transacylase activity, but significant success has been achieved more in the acylation than in the deacylation step.<sup>27</sup> It appears, therefore, that the supramolecular complex (7)  $\text{Ba}^{2+}$  can be viewed as a prototype catalyst, from which it is hoped that more sophisticated structures capable of displaying enzyme-like transacylase activity can be derived.

## 6 Concluding Remarks

The results presented in this account show to what an extent the rates of reactions of anionic nucleophiles with neutral molecules, including their intramolecular versions, are influenced by alkali and alkaline-earth metal ions. Rate effects measured under carefully controlled conditions span over 12 orders of magnitude, ranging from the  $10^{-5}$  rate inhibition observed in the alkylation of the magnesium derivative of  $\beta$ -ketoenolates to the  $10^7$  rate enhancement found in the cleavage of the barium complex of *p*-tert-butylcalix[4]arene-crown-5 monoacetate. Discussion has been focused on transition state stabilization by metal ions, and on the beneficial influence of additional binding energy rendered available by a polyether moiety proximal to the reaction zone. Our work in this field widens considerably the scope of group 1 and group 2 metal ions as effective catalysts of

transacylation processes, which have potential for further investigation and development in the field of supramolecular catalysis

*Acknowledgements* The contributions of the colleagues whose names appear in the cited references are deeply acknowledged

## 7 References

- 1 'Crown Ethers and Analogs', ed S Patai and Z Rappoport, J Wiley New York, 1989, G Gokel, 'Crown Ethers and Cryptands', The Royal Society of Chemistry, Cambridge, 1991
- 2 R M Izatt, K Pawlak, J S Bradshaw, and R L Bruening, *Chem Rev*, 1991, **91**, 1721
- 3 G Illuminati and L Mandolini, *Acc Chem Res*, 1981, **14**, 95, L Mandolini, *Adv Phys Org Chem*, 1986, **22**, 1
- 4 D N Reinhoudt and F de Jong, in 'Progress in Macrocyclic Chemistry', ed R M Izatt and J J Christensen, J Wiley and Sons, New York, 1979, vol 1, p 176
- 5 L Mandolini, *Pure and Appl Chem*, 1986, **58**, 1485
- 6 L Mandolini and B Masci, *J Am Chem Soc*, 1977, **99**, 7709
- 7 (a) G Illuminati, L Mandolini, and B Masci, *J Am Chem Soc*, 1983, **105**, 555, (b) L Mandolini and B Masci, *J Am Chem Soc*, 1984, **106**, 168
- 8 (a) G Ercolani, L Mandolini, and B Masci, *J Am Chem Soc*, 1981, **103**, 2780, (b) 1981, **103**, 7484, (c) 1983, **105**, 6146
- 9 J E Gordon, 'The Organic Chemistry of Electrolyte Solutions', J Wiley, New York, 1975
- 10 (a) M Crescenzi, C Galli, and L Mandolini, *J Chem Soc Chem Commun*, 1986, 551, (b) *J Phys Org Chem*, 1990, **3**, 428, (c) C Galli and L Mandolini, *J Chem Soc Perkin Trans 2*, 1984, 1435, (d) R Cacciapaglia and L Mandolini, *J Org Chem*, 1988, **53**, 2579, (e) *Tetrahedron*, 1990, **46**, 1353
- 11 A Ostrowicki, E Koepp, and F Vogtle, *Top Curr Chem*, 1992, **161**, 37
- 12 C Galli and L Mandolini, *J Org Chem*, 1991, **56**, 3045, C Galli, *Org Prep and Proc Int*, 1992, **24**, 285
- 13 C Antonini Vitali and B Masci, *Tetrahedron*, 1989, **45**, 2213
- 14 G Ercolani and L Mandolini, *J Am Chem Soc*, 1990, **112**, 423
- 15 M J Pregel and E Buncel, *J Org Chem*, 1991, **56**, 5583 and previous papers in the series. See also K J Msayib and C I F Watt *Chem Soc Rev*, 1992, **2**, 237
- 16 G Dodd, G Ercolani, P Mencarelli, and C Scalamandre, *J Org Chem*, 1991, **56**, 6331
- 17 (a) R Cacciapaglia, S Lucente, L Mandolini, A R van Doorn, D N Reinhoudt, and W Verboom, *Tetrahedron*, 1989, **45**, 5293, (b) R Cacciapaglia, A R van Doorn, L Mandolini, D N Reinhoudt and W Verboom, *J Am Chem Soc*, 1992, **114**, 2611
- 18 D Kraft, R Cacciapaglia, V Bohmer, A A El-Fadl, S Harkema, L Mandolini, D N Reinhoudt, W Verboom, and W Vogt, *J Org Chem*, 1992, **57**, 826
- 19 R Cacciapaglia, L Mandolini, D N Reinhoudt, and W Verboom, *J Phys Org Chem*, 1992, **5**, 663
- 20 J-M Lefour and A Loupy, *Tetrahedron*, 1978, **34**, 2597
- 21 L P Hammett, 'Physical Organic Chemistry', McGraw-Hill, New York, 1970, p 118
- 22 R Cacciapaglia, L Mandolini, and F S Romolo, *J Phys Org Chem*, 1992, **5**, 457
- 23 R Cacciapaglia, L Mandolini, and V Van Axel Castelli, *Recl Trav Chim Pay-Bas*, 1993, **112**, 347
- 24 R Cacciapaglia, A Casnati, L Mandolini, and R Ungaro, *J Chem Soc Chem Commun*, 1992, 1291
- 25 R Cacciapaglia, A Casnati, L Mandolini, and R Ungaro, *J Am Chem Soc*, 1992, **114**, 10956
- 26 A Fersht, 'Enzyme Structure and Mechanism', W H Freeman and Co, New York, 1985, Chapter 4
- 27 (a) R Breslow, G Trainor, and A Ueno, *J Am Chem Soc*, 1983, **105**, 2739, (b) D J Cram, P Y -S Lam, and S P Ho, *J Am Chem Soc*, 1986, **108**, 839, (c) J M Lehn and C Sirlin, *New J Chem*, 1987, **11**, 693, (d) J Suh, *Bioorg Chem*, 1990, **18**, 345, (e) F Diederich, 'Cyclophanes', The Royal Society of Chemistry, Cambridge, 1991, Chapter 8, (f) J Murakami, J Kikuchi, and Y Hisaeda, 'Inclusion Compounds', ed J L Atwood, J E D Davies, and D D Mac Nicol, Oxford University Press, New York, 1991, Vol 4, Chapter 11